# Fluidics Behavior During Vitrectomy

We explain the effect of high-speed cutting on flow rates, peak velocities, and peak accelerations in laboratory experiments and their relevance to clinical surgery.

BY DINA ABULON; MS, DAVID BUBOLTZ, BS, MBA; AND STEVE CHARLES, MD

dvancements in vitreoretinal instrumentation have expanded the selection of surgical parameters during vitrectomy procedures. With numerous combinations of system settings, the task of optimizing aspiration flow rates while maintaining precise tissue cutting can be challenging. To safely utilize new-generation instruments, surgeons should understand fluidic behavior during vitrectomy.

Poiseuille's law can be used to describe flow rate through a vitrectomy probe (see Equation 1). The variable R is the inner lumen radius, P is the pressure drop across the cutter,  $\mu$  is the dynamic viscosity of aspirated fluid, and I is the length of cylindrical tubing through which flow is measured. Poiseuille's equation is valid for laminar flow of an incompressible fluid such as balanced salt solution through the probe when the cutter is disabled. Under realistic surgical conditions, the heterogeneous composition of vitreous complicates fluid dynamics. Although the nature of vitreous behavior during aspiration is complex, the relationship between flow rate, probe geometry, applied vacuum pressure, and viscosity of aspirated fluid still provide insight into fluid dynamics during vitrectomy.

(Equation 1). Flow Rate = 
$$Q = \frac{\pi R^4 \Delta P}{8\mu l}$$

The evolution of probe design continues to expand the variety of surgical parameters governing flow rate. Vitreous surgery was originally performed using 20-gauge pneumatic, spring-return cutters.<sup>2</sup> Design improvements, such as reduced outer probe diameter, led to 23- and 25-gauge transconjunctival sutureless vitrectomy instruments that reduced sclerotomy inflammation.<sup>3,4</sup> Although smaller-diameter instruments improved postoperative patient comfort, surgeons experienced reduced flow rates during vitrectomy.<sup>4,5</sup> Spring-return mechanisms were engineered to achieve maximum cut speeds of 2500 cpm and demonstrated

# WATCH IT ON NOW ON THE RETINA SURGERY CHANNEL AT WWW.EYETUBE.NET

The Effect of High Cutting Rates on Flow Rates, Peak Velocities, and Accelerations in Porcine Eyes and Clinical PPV



By Steve Charles, MD direct link to video: http://eyetube.net/?v=fared



increased vitreous flow rates at higher cut rates.<sup>6,7</sup> Now, new-generation cutters operate using a dual pneumatic drive rather than spring-return mechanism which allows the cutter to achieve even higher cut rates of 5000 cpm and to modulate duty cycle or percent of port open time. The dual pneumatic probe technology has introduced higher cut rate capabilities and a variety of duty cycle settings that may affect surgical technique and flow behavior during surgery.

As previous studies evaluated flow performance of spring-return cutters at the maximum cut rate of 2500 cpm, it is important to evaluate the performance of new generation cutters at 5000 cpm and at various duty cycle modes. In this study, two laboratory bench tests were performed to determine the effects of high speed cutting on flow rates during vitrectomy. The purpose of the first test was to measure flow rates in pure porcine vitreous at various cut rates. The purpose of the second test was to measure the peak velocity and peak acceleration of clear fluid flow into the probe port.

# EXPERIMENT 1: PORCINE VITREOUS FLOW Purpose

The purpose of the first experiment was to investigate porcine vitreous flow performance of 23-gauge UltraVit probes (Alcon Laboratories, Inc., Fort Worth,

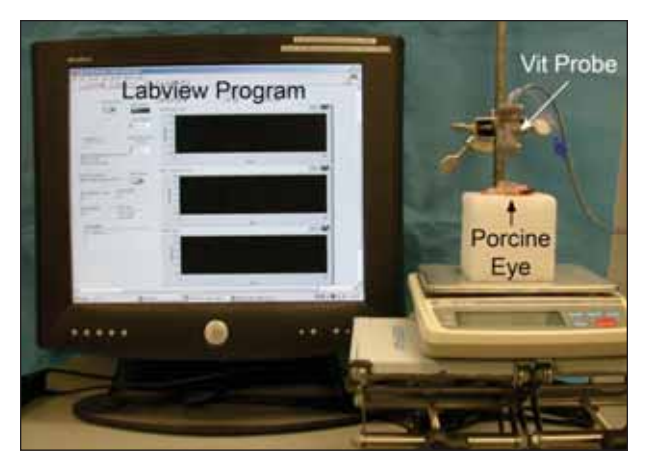


Figure 1. Test set up for porcine vitreous flow measurements.

TX) at various duty cycle modes, cut speeds, and vacuum pressures.

### Methods

A Constellation Vision System (Alcon Laboratories, Inc.) was used to test six dual-pneumatic UltraVit probes. Three duty cycle modes were evaluated with the vitrectomy system: core (maximum port open time), 50% port open, and shave (minimum port open time). Each probe was tested at vacuum settings of 250 mm Hg, 450 mm Hg, and 650 mm Hg and at cut rates of 500 cpm to 5000 cpm.

Porcine eyes from Sierra for Medical Science (Whittier, CA) were tested within 48 hours of slaughter. Each eye was kept refrigerated until immediately before testing. Prior to flow rate testing, vitreous density was measured by weighing the mass of 3 mL to 4 mL of extracted vitreous in a previously weighed graduated cylinder. Density measurements were repeated for 10 eyes and averaged.

A Styrofoam cube with 3-inch edges was used as a mount for the porcine eyes. A spherical recess 1 inch in diameter was created on the top of the cube to secure the eye. Multiple T-pins were used to fasten one eye in the spherical recess with the cornea facing upward. Using a scalpel, an initial incision was made through the pars plana, 3 mm from the limbus. The initial incision was extended in an annulus around the cornea and the anterior chamber of the eye was removed. Any vitreous attachments to the posterior capsule were carefully detached using the scalpel. The Styrofoam block with the porcine eye secured into it was placed on an electronic balance (model EK-600i, A&D Engineering, Inc., San Jose, CA). The vitrectomy probe to be tested was secured vertically over the balance using a clamp and lab stand. The vitrectomy probe port was inserted into the center of the vitreous bolus. One porcine eye was used per test.

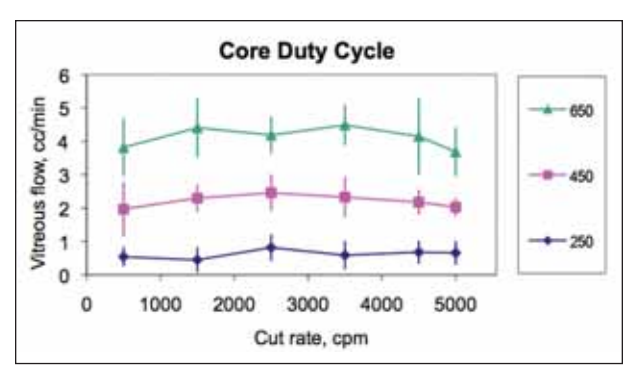


Figure 2. 23-gauge Vitreous flow in core duty cycle mode.

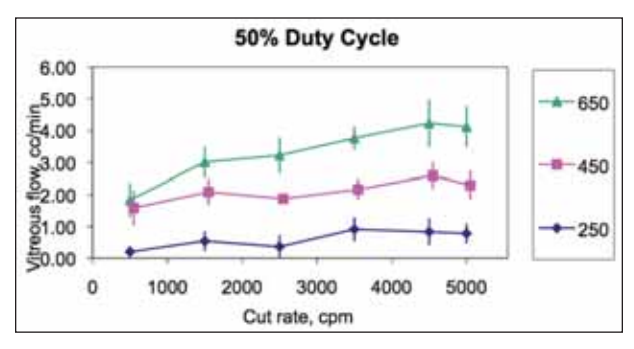


Figure 3. 23-gauge Vitreous flow in 50% duty cycle mode.

The electronic balance was connected directly to a personal computer using a RS232 cable (Figure 1). A LabVIEW program (National Instruments, Austin, TX) was written to measure mass with time. Volume flow rates were calculated using previously obtained vitreous density measurements. The LabVIEW program divided the mass flow by the average porcine vitreous density. Volume flow data was exported from the program as a Microsoft Excel file. Prior to each test, the balance was zeroed and the appropriate Constellation Vision System settings were chosen. LabVIEW data capture was activated after the vitreous cutter was engaged and vitreous flow stabilized (after ~5 seconds).

Vitreous flow rates were compared with previously presented flow rates of balanced salt solution (BSS irrigating solution, Alcon Laboratories, Inc.).8 For BSS flow tests, key differences in experimental set up included a closed-globe, rigid model eye; applied infusion pressure of 30 mm Hg; and a flow meter instead of an electric balance.

For each test, the vitreous flow rate was calculated as the average of data points after the initial time to stabilize and before all vitreous was removed from the eye. All data are presented as mean  $\pm$  standard deviation unless otherwise noted. Flow rates were compared using Student's t-test with statistical significance of P < .05. Trend lines were examined by linear regression

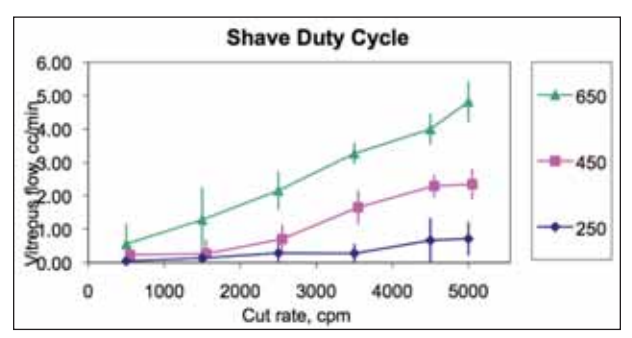


Figure 4. 23-gauge Vitreous flow in shave duty cycle mode.

and correlation coefficients were calculated using Microsoft Excel.

### Results

Figures 2 to 4 depict vitreous flow rates through 23-gauge UltraVit probes at the 3 duty cycle modes of the Constellation Vision System. Each data point on the graph illustrates the average flow rate of six probes and error bars represent 95% confidence intervals.

Core Duty Cycle. The core duty cycle mode generated relatively stable vitreous flow rates across all cut rates and vacuums (R2 $\leq$ .2). For all vacuum pressures, there was no significant difference between flow at the minimum and maximum tested cut speeds of 500 cpm and 5000 cpm. In the core mode, flow at low cut rates were significantly higher than flow at low cut rates in of the 50% and shave modes at equivalent settings (P<.05). A maximum flow rate of 3.69  $\pm$  0.92 cc/min was achieved at 650 mm Hg vacuum and 5000 cpm.

50% Duty Cycle. In the 50% duty cycle mode, flow increased with increasing cut rate. For all vacuum pressures, flow at 5000 cpm was significantly higher than flow rates at 500 cpm (P<.05). At 50% duty cycle, 450 and 650 vacuum, low cut rate (500 cpm), flow was significantly higher than shave (P<.05). Minimum vacuum and cut rate settings (250 mm Hg vacuum and 500 cpm) generated flow rates of 0.20  $\pm$  0.19 cc/min. Maximum flow of 4.12  $\pm$  0.81 cc/min was achieved at maximum vacuum and cut rate settings (650 mm Hg and 5000 cpm). Maximum flow was statistically similar to flow in the core and shave duty cycle at equivalent settings.

Shave Duty Cycle. Flow in the shave mode increased with increasing cut rate. For all vacuum settings, flow rate at 5000 cpm was significantly higher than 500 cpm (P<.05). Flow in the shave mode increased more rapidly than flow of 50% duty cycle. For 50% duty cycle, the slope of trend lines for 250 mm Hg, 450 mm Hg, and 650 mm Hg vacuum were 0.1µL/cut, 0.2 µL/cut, and 0.5 µL/cut, respectively (all R2 $\geq$ .7). For shave duty cycle,

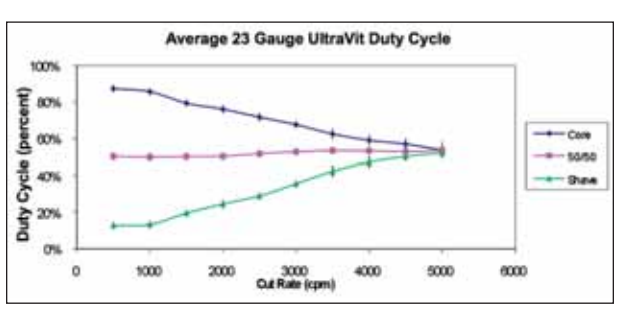


Figure 5. 23-Gauge duty cycle.

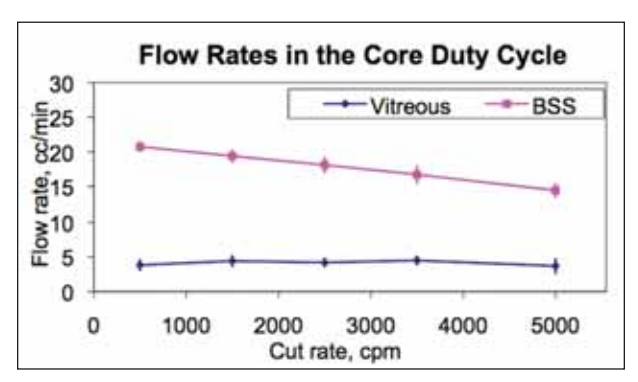


Figure 6. 23-gauge Vitreous and BSS flow rates at 650 mm Hg vacuum and core duty cycle.

slope of trend lines for 250 mm Hg, 450 mm Hg, and 650 mm Hg vacuum were 0.2  $\mu$ L/cut, 0.5  $\mu$ L/cut, and 0.9  $\mu$ L/cut, respectively (all R2 $\geq$ .9). At maximum vacuum and cut rate (650 mm Hg and 5000 cpm), flow was statistically similar to flow in the core mode at equivalent settings. For the shave mode, flow rates ranged from 0.05  $\pm$  0.12 cc/min (at 250 mm Hg vacuum and 5000 cpm) to a maximum flow rate of 4.82  $\pm$  0.77 cc/min (at 650 mm Hg vacuum and 5000 cpm).

Vitreous flow of 23-gauge UltraVit probes in the core mode was not strongly dependent on cut rate; flow remained relatively constant for all cut rates. Vitreous flow in the 50% and shave duty cycle modes was influenced by cut rate; flow increased with increasing cut rate. The rate of increase for the shave mode was higher than that of the 50% duty cycle. At the maximum vacuum and cut-rate settings, flow rates were statistically similar for all duty cycle modes.

### DISCUSSION

This study demonstrated the effects of cut rate, duty cycle, and vacuum on vitreous flow rates. Figure 5 illustrates the average duty cycle of six 23-gauge UltraVit cutters. Figures 6 to 8 compare the findings of this study to the average clear fluid flow rates of six 23-gauge UltraVit® cutters operating at 650 mm Hg vacuum and 500-5000 cpm. Error bars illustrate a

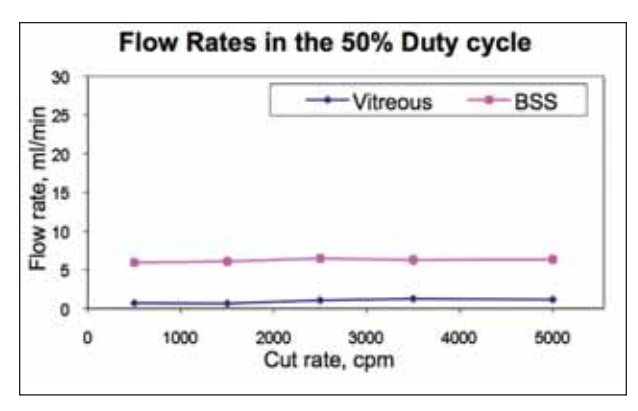


Figure 7. 23-gauge Vitreous and BSS flow rates at 650 mm Hg vacuum and 50% duty cycle.

confidence interval of 95%.

Core Duty Cycle. At 500 cpm, the core duty cycle of the Constellation Vision System generated a maximum of  $87.34 \pm 0.86\%$  duty cycle that decreased to 53.63± 1.82% at 5000 cpm.9 It was reported that clear fluid flow generated a maximum flow rate of 20.8  $\pm$  0.9 cc/min at low cut rates (500 cpm) that decreased to 14.45 ± 1.32 cc/min at higher cut rates (5000 cpm).8 Both clear fluid flow rates and duty cycle decreased with increasing cut rate in the core mode. Since aqueous flow and core duty cycle are dependent on cut rate, we might expect to see a decrease in vitreous flow as cut rate increases; however, vitreous exhibited constant flow at all cut rates (Figure 7). High cut rates fragment vitreous into smaller segments resulting in reduced flow obstructions.<sup>10</sup> Conversely, low cut rates generate less vitreous fragmentation and more flow obstruction due to the reduced cut frequency. At low cut rates, the effects of high duty cycle may have offset reduced vitreous flow (from decreased fragmentation) resulting in constant flow rates for all cut speeds. In other words, constant vitreous flow in the core duty cycle mode suggests that there is an increased resistance to flow at low cut rates.

50% Duty Cycle. In the 50/50 mode, clear fluid flow rates reflect the constant duty cycle and maintain relatively constant flow ranging from  $13.58 \pm 0.37$  to  $14.3 \pm 0.83$  cc/min at 500 cpm to 5000 cpm, 650 mm Hg vacuum (Figure 9). Puring 50% duty cycle, the port open time proportionally decreases with increasing cut rate in order to maintain a constant 50% duty cycle for all cut rates. The duration of port open time is longer at lower cut rates than higher cut rates, but the ratio of port open time to cut cycle time remains 50% for all cut rates. We might expect vitreous flow to maintain constant flow similar to clear fluid behavior, but vitreous flow rates increased from  $1.83 \pm 0.68$  (500 cpm) to

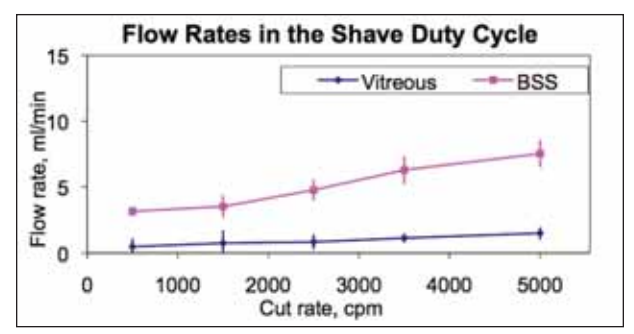


Figure 8. 23-gauge Vitreous and BSS flow rates at 650 mm Hg and shave duty cycle.

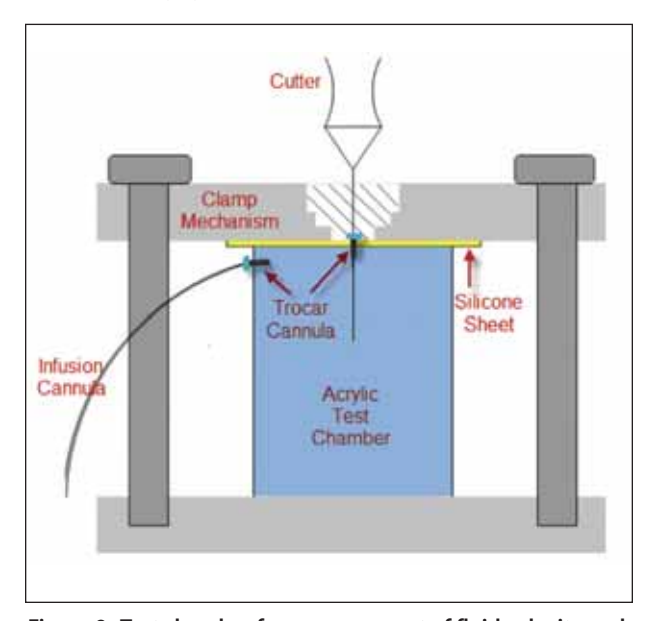


Figure 9. Test chamber for measurement of fluid velocity and acceleration.

 $4.12\pm0.81$  cc/min (5000 cpm), suggesting that the decreased port open time at high cut rates is associated with reduced aspirated volume, increased vitreous fragmentation, and reduced flow resistance.

Shave Duty Cycle. The shave duty cycle maintained a constant port open time for all cut rates. Recall that duty cycle was defined as the percent ratio of port open time to cut cycle time. With increasing cut rate, the port open time was held constant while cut cycle time decreased resulting in a duty cycle that climbed from  $12.80 \pm 1.05\%$  to  $52.15 \pm 1.06\%$ . Aspiration during one cut cycle can be described as a cut "bite" where vacuum pressure draws vitreous into the open port and the guillotine cutter fragments and aspirates a discrete volume of vitreous. Because the port open time is equivalent for all cut rates, the shave duty cycle behavior suggests the discrete volume of vitreous aspirated per cut bite is also equivalent for all cut rates. If the

frequency of these cut bites increase at high cut rates, then the amount of aspirated vitreous fragments also increases with high cut rates. Thus, increased vitreous flow may be associated with high cut rates in the shave duty cycle as the probe engages vitreous more frequently than low cut rates. This study demonstrated an increase in vitreous flow at 650 mm Hg vacuum from  $0.59 \pm 0.76$  cc/min at 500 cpm to  $4.82 \pm 0.77$  cc/min at 5000 cpm (Figure 8). Although the shave duty cycle maintained an equivalent cut bite size for all cut rates, increased vitreous flow and increased intake of cut bites (associated with high cut rates) suggests that vitreous aspiration is more effective at high cut rates.

It is important to address the difference in test methods between vitreous and clear fluid flow data. Vitreous flow rates were captured using an electronic balance to measure open-sky vitrectomy rates while aqueous flow data was collected using a BSS infusion flow meter in a rigid, closed-system eye model. A closed system can be pressurized—an open system cannot. Although the pressure response differs between the two systems, both experimental methods generate measurements that help characterize flow rates during vitrectomy. Another important difference to note is the composition of aspirated materials. The heterogenous properties of vitreous drastically differ from BSS irrigating solution. Vitreous is a semisolid mixture of water, collagen fibers, and hyaluronic acid. The complex nature of vitreous is unpredictable during vitrectomy and can sometimes generate a high standard deviation due to vitreous flow obstructions. Clear fluid flow tests were repeatable, predictable, and more accurately reflect Poiseuille's law of flow. Despite differences in the composition of aspirated fluids, a comparison between clear fluid and vitreous helps characterize vitrectomy flow behavior.

# CONCLUSION

In summary, the 50% duty cycle mode generated an increase in vitreous flow at high cut rates suggesting that high cut rates generate less flow resistance. Constant vitreous flow in the core duty cycle mode across all cut rates implies that the high flow effects of the core duty cycle are offset by the increased resistance to vitreous flow associated with larger bite sizes. In the shave mode, vitreous flow increased at high cut rates as the frequency of constant-volume bites increased with high cut rates. Overall, the operation of 23-gauge UltraVit probes at high cut rates yielded reduced resistance to flow at high cut rates and more effective aspiration of the vitreous body than lower cut rates.

# EXPERIMENT 2: MEASUREMENT OF PEAK FLOW VELOCITY AND PEAK ACCELERATION

# **Purpose**

The purpose of the second experiment was to determine the effects of cut rate on peak flow velocity and peak acceleration of clear fluid and microbeads through 25+-gauge dual-pneumatic cutters.

# Methods

A Constellation Vision System was used to test an UltraVit probe in a closed-system, test chamber. Flow was evaluated at 5000 cpm, 650 mm Hg vacuum and at 2500 cpm, 575 mm Hg vacuum to achieve equivalent flow rates of approximately 7 cc/min. All testing was performed under 30 mm Hg infusion pressure and 50% duty cycle.

The test chamber was designed to simulate the closed system of a compliant human eye while allowing for visualization of fluid entering the probe port. The test chamber was a 1x1x2-inch open box made of clear acrylic. A square 1.5-inch silicone sheet of 0.005-inch thickness with a reading of 55A durometer was used to cover and seal the box (McMaster-Carr, Santa Fe Springs, CA). The silicone sheet was secured over the top of the acrylic test chamber using a metal clamping mechanism (Figure 12). The flexible properties of the silicone cover simulated the dampening effect of compliant sclera. The test chamber was filled with aqueous solution and 75 µm microbeads were injected to help visualize fluid motion during aspiration.

To replicate fluid input and output during vitrectomy, the test chamber was modified to incorporate to two trocar cannula entry ports—one for BSS fluid infusion and a second port for the vitrectomy probe. A 0.02-inch diameter hole was drilled in the side wall of the test chamber. A 25+-gauge trocar cannula (Alcon Laboratories Inc.) was secured in the drilled hole using Loctite 4014 (Henkel, Berkeley, CA). A 25+ infusion cannula (Alcon Laboratories Inc.) was inserted into the 25+-gauge trocar cannula and supplied BSS infusion to the test chamber. A second port was created by inserting a 25+-gauge trocar cannula into the silicone cover using the 25+-gauge trocar blade. The vitrectomy probe to be tested was secured vertically over the test chamber using a three-screw adjustable ring mount (Edmund Optics, Barrington, NJ). The probe tip was inserted into the test chamber through the second entry port of the silicone cover and centered in the test chamber.

Two different camera perspectives were required for 3-D motion analysis. Two Phantom high-speed cameras (Vision Research, Wayne, NJ) were oriented orthogonally around the test chamber. Each camera was secured to an Edmund Optics X-Y-Z axis metric stage for precise

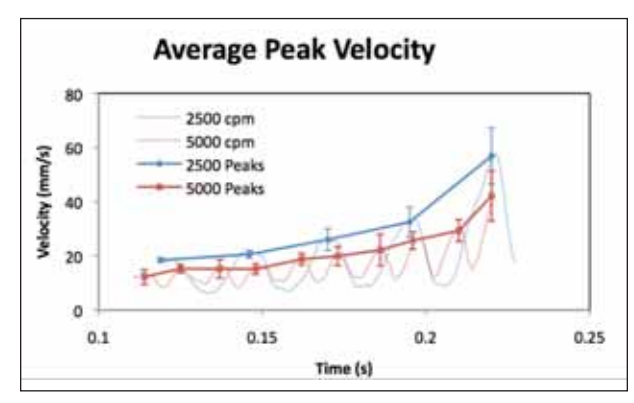


Figure 10. Average 25+-gauge peak flow velocity of microbeads in BSS (50% duty cycle, 7cc/min flow rate).

position adjustment. A Computar 10X magnification lens was fastened to each camera and focused on the vitrectomy probe port. Two fluorescent backlight panels illuminated the test chamber.

Both cameras were tethered to one another in a master and slave configuration to synchronize recording. An external pickle switch was connected to both cameras in order to manually trigger video recording at the same time. Both cameras were directly connected to a personal computer with an Ethernet cable. High-speed video was recorded at 1000 frames per second. The video resolution for each camera was 640x480 pixels. Brightness, contrast, and exposure time was adjusted to clearly define microbeads around the probe port.

Prior to high-speed recording, the appropriate Constellation Vision System settings were chosen. An infusion pressure of 30 mm Hg was applied to the test chamber. Video capture was triggered with the pickle switch after the cutter was engaged and fluid flow stabilized. Recording was stopped after approximately 20 seconds of recording and each camera saved an audio video interleave (AVI) file.

Prior to video analysis, 3-D measurements of TEMA Motion Software (Photo-Sonics Inc, Burbank, CA) were calibrated. Relative camera orientations were manually entered into the program. Six points on a calibration target visible from both cameras were identified. The software translated 2-D measurements from each camera into 3-D motion. During analysis, AVI video files of each camera perspective were imported into the TEMA software program. Each file was synchronized and viewed simultaneously in the analysis window. Individual microbeads were manually selected from each perspective and the software tracked microbead motion into the vitrectomy probe port frame-by-frame. Velocity and acceleration data was exported from the program as a Microsoft Excel file. Peak velocity and

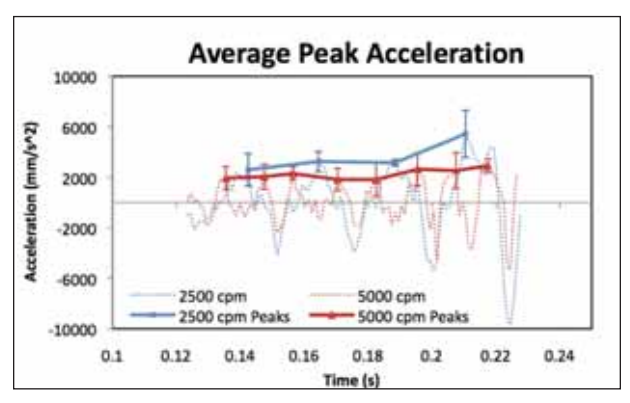


Figure 11. Average 25+-gauge peak acceleration of microbeads in BSS (50% duty cycle, 7cc/min flow rate).

peak acceleration values of five tracked microbeads were averaged for each cut rate. All data are presented as mean  $\pm$  standard deviation. Velocities and accelerations were compared using a two-tailed, Student's t-test with statistical significance of P<.05.

## RESULTS

Figure 10 and 11 depict peak velocity and peak acceleration graphs of microbeads entering a 25+-gauge UltraVit cutter at 2500 cpm and 5000 cpm, 50% duty cycle. Each data point on Figure 10 illustrates the average peak velocity of 5 microbeads during aspiration into the vitrectomy probe port. Each data point in Figure 11 illustrates the average peak acceleration of five microbeads. The time axis of Figures 10 and 11 can relate to microbead distance from the port and range from 0.1 to 0.25 for clear illustration of velocity and acceleration profiles. Error bars represent 95% confidence intervals.

At 2500 cpm, the average peak velocity of microbeads increased as the beads approached the port. Just immediately before entering the probe port, the average maximum peak velocity was 52.98  $\pm$  11.89 mm/s. With 5000 cpm cut rate and vacuum pressure of 650 mm Hg, the average peak velocity also increased with time. The average maximum peak velocity before aspiration into the probe port was 42.06  $\pm$  10.51 mm/s. Statistical evidence suggests that peak velocities during aspiration at 2500 cpm were significantly higher than 5000 cpm (P<.05). On average, peak velocities occurring at 2500 cpm were approximately 24.28% faster than 5000 cpm peak velocities.

For 2500 and 5000 cpm cut rates, the average peak acceleration increased as the beads approached the port. Maximum peak acceleration of microbeads reached  $\pm 1479.84$  mm/s2 prior to entering the probe port. At 5000 cpm, peak accelerations reached an average

value of 2909.88  $\pm$  538.82 mm/s². Statistical evidence suggests that aspiration at 2500 cpm generated significantly higher average peak accelerations than beads aspirated at 5000 cpm (P<.05). Average acceleration for 2500 cpm cut speeds generated approximately 34.80% higher peak acceleration values than 5000 cpm cut speeds.

Aspiration with the 25+-gauge UltraVit probe demonstrated an increase in velocity and acceleration as beads approached the port for both 2500 and 5000 cpm. The 2500 cpm cut rate generated faster peak flow velocities and higher peak accelerations than 5000 cpm.

# **DISCUSSION**

This study demonstrated the effects of cut rate on peak velocity and peak acceleration of fluid in a closed-system test chamber. We evaluated the motion of 5 microbeads into an UltraVit 25+-gauge probe at 2500 cpm, 575 mm Hg vacuum and 5000 cpm, 650 mm Hg vacuum. All testing was performed under 50% duty cycle and 30 mm Hg infusion.

During a cut cycle, the velocity of fluid increases and decreases according to port open and close times. When the port is fully open, fluid reaches peak velocity. This velocity can be directly related to flow using a basic principle of volume flow rate: Flow rate = orifice area x fluid velocity. Reduced peak velocity at high cut rates translates into reduced clear fluid flow at high cut rates. Under surgical conditions, reduced peak flow velocities and flow rates of BSS suggests that operation at 5000 cpm may reduce pulsatile disturbance of tissue and fluid in the eye. The data shows fluid and microbeads aspirated at 2500 cpm approached the probe port with 24.28% faster peak velocity than 5000 cpm.

According to Newton's second law relating acceleration and inertial mass to force (Force = mass x acceleration), lower acceleration leads to reduced forces on fluid and tissue around the port. As high cut rate yields lower aspiration forces at the probe port, surgeons can precisely operate closer to the surface of tissue and membranes, reduce vitreoretinal traction, and reduce the incidence of iatrogenic retinal breaks. Data analysis of fluid acceleration demonstrated that higher cut rates generated lower accelerations and associated forces, as peak accelerations at 5000 cpm were 34.80% lower than 2500 cpm.

Limitations of this study included a test chamber design that did not perfectly replicate the conditions in a human eye. The rigid test chamber does not exhibit the same flexibility and dampening as scleral tissue. Although reported measurements using the rigid model may not exactly represent testing in an eye, a silicone wall of the test chamber was used to replicate some degree of tissue compliance.

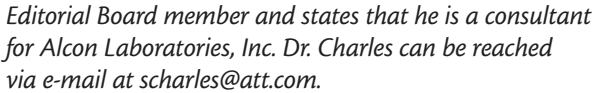
# CONCLUSIONS

The first test measured flow rates of porcine vitreous at various cut rates and duty cycle settings. Results indicated higher vitreous flow at high cut rates suggesting reduced flow resistance and more efficient vitreous aspiration. The second test measured peak flow velocities and peak accelerations of microbeads and BSS fluid entering the vitrectomy probe port. It was determined that 2500 cpm generated faster peak velocities and higher peak accelerations than 5000 cpm. This suggests that high cut rate reduces BSS fluid flow and hence, reduces aspiration forces, pulsatile vitreoretinal traction, and iatrogenic tears while allowing for more precise control of fluid surrounding the port.

Overall, high cut rates of dual pneumatic probes generated clinically effective vitreous flow and reduced aspiration forces. By investigating the effects of high cutting rates on vitreous and clear fluid, this study characterizes flow behavior of advanced probe technology and helps surgeons optimize system settings to improve the efficiency and precision of surgical technique.

Dina Abulon, MS; and David Buboltz, BS, MBA, are with Alcon Laboratories in Fort Worth, TX.

Steve Charles, MD, is Founder of the Charles Retina Institute in Memphis, TN, and is a Clinical Professor in the Department of Ophthalmology at the University of Tennessee College of Medicine. He is a Retina Today



- Munson BR. Fundamentals of Fluid Mechanics. New York: John Wiley & Sons, Inc. 2002.
  O'Malley C, Heintz R. Vitrectomy with an alternative instrument system. *Ann Ophthalmol*. 1975;585-588, 591-594.
- Eckardt, C. Transconjunctival sutureless 23-gauge vitrectomy. Retina. 2005;25:208-211.
  Didi FI, Moisseiev J. Sutureless vitrectomy: evolution and current practices. Br J Ophthalmol. 2010 Aug 23. [Epub ahead of print)
- 5. Hubschman JP, Gupta A, Bourla D. Culjat M, Schwartz SD. 20-, 23-, and 25-gauge vitreous cutters: performance and characteristics evaluation. *Retina*. 2008;249-257.
- 6. Magalhaes O, Chong L, DeBoer C, et al. Vitreous flow analysis in 20-, 23-, and 25-gauge cutters. Retina. 2008;236-241.
- Ho, A. Next generation vitrectomy technology for microincision vitrectomy surgery.
  Presented at the Retina Congress; September 30-October 4, 2009; New York, NY.
- 8. Novack, R. Relationship of duty cycle versus cut rate for two commercially available systems. Presented at: the American Society of Retina Specialists' 28th Annual Meeting; August 26-September 1, 2010; Vancouver, Canada.
- Teixeira A, Chong L, Matuoka N, et al. An experimental protocol of the model to quantify traction applied to the retina by vitreous cutters. *Invest Ophthalmol Vis Sci.* 2010;4181-4186.

# **CONTACT US**

Send us your thoughts via e-mail to letters@bmctoday.com.